SCIENCE CHINA
Life Sciences

Tsinghua Special Issue
• RESEARCH PAPER •

January 2014 Vol.57 No.1: 11–21
doi: 10.1007/s11427-013-4587-9

Arabidopsis co-chaperonin CPN20 antagonizes Mg-chelatase H subunit to derepress ABA-responsive WRKY40 transcription repressor

ZHANG XiaoFeng†, JIANG Tao†, YU YongTao, WU Zhen, JIANG ShangChuan, LU Kai, FENG XiuJing, LIANG Shan, LU YanFen, WANG XiaoFang* & ZHANG DaPeng*

MOE Systems Biology and Bioinformatics Laboratory, School of Life Sciences, Tsinghua University, Beijing 100084, China

Received October 14, 2013; accepted November 20, 2013; published online December 23, 2013

Our previous study demonstrated that a chloroplast co-chaperonin 20 (CPN20), one of the interaction partners of the magnesium-protoporphyrin IX chelatase H subunit (CHLH/ABAR), negatively regulates ABA signaling at the same node with ABAR but upstream of WRKY40 transcription repressor in *Arabidopsis thaliana*. In the present experiment, we showed that ABA directly inhibits the ABAR-CPN20 interaction, and also represses expression of *CPN20*, which depends on ABAR. CPN20 inhibits ABAR-WRKY40 interaction by competitively binding to ABAR. ABAR downregulates, but CPN20 upregulates, *WRKY40* expression. The *cpn20-1* mutation induces downregulation of *WRKY40*, and suppresses the upregulated level of *WRKY40* due to the *cch* mutation in the *ABAR* gene. ABA-induced repressive effect of the *WRKY40* gene is strengthened by downregulation of *CPN20* but reduced by upregulation of *CPN20*. Together with our previously reported genetic data, we provide evidence that CPN20 functions through antagonizing the ABAR-WRKY40 coupled pathway, and ABA relieves this pathway of repression by inhibiting the ABAR-CPN20 interaction to activate ABAR-WRKY40 interaction.

co-chaperonin, CPN20, Mg-chelatase H subunit, WRKY40, ABA signalling

Citation: Zhang XF, Jiang T, Yu YT, Wu Z, Jiang SC, Lu K, Feng XJ, Liang S, Lu YF, Wang XF, Zhang DP. *Arabidopsis* co-chaperonin CPN20 antagonizes Mg-chelatase H subunit to derepress ABA-responsive WRKY40 transcription repressor. Sci China Life Sci, 2014, 57: 11−21, doi: 10.1007/s11427-013-4587-9

Phytohormone abscisic acid (ABA) regulates many developmental processes including embryo maturation, seed germination and seedling growth, and is a key hormone in plant adaptation to adverse conditions such as drought, salt and cold stresses [1−3]. ABA signal transduction has been extensively studied, and numerous signaling components, including several receptors or candidate receptors for ABA, have been identified [1,3−10].

We previously reported that the chloroplast magnesium-protoporphyrin IX chelatase large subunit (Mg-chelatase H subunit CHLH/putative ABA receptor ABAR) functions as a candidate receptor for ABA in *Arabidopsis thaliana* [4,11,12], which antagonizes a group of WRKY-domain transcription repressors to relieve ABA-responsive genes of inhibition [13−15]. Although the identity of CHLH/ABAR as an ABA receptor is controversial [16], multiple lines of evidence showed that CHLH/ABAR binds ABA and functions in ABA signaling [4,11−13,17]. Further evidence revealed that CHLH/ABAR mediates ABA signaling in guard cells of several plant species such as *Arabidopsis* [4,16,18], peach (*Prunus persica*) [19], and tobacco (*Nicotiana benthamiana*) [12]. Additionally, CHLH/ABAR mediates ABA signaling in fruit ripening of both peach [19]

†Contributed equally to this work
*Corresponding author (email: zhangdp@tsinghua.edu.cn; wangxf@biomed.tsinghua.edu.cn)

and strawberry (*Fragaria ananassa*) [20]. These data demonstrate that CHLH/ABAR is an essential ABA signaling regulator in plant cells.

Recently, we showed that the chloroplast co-chaperonin CPN20 interacts with ABAR/CHLH protein, and negatively regulates ABA signaling at the same node with ABAR and upstream of the WRKY40 transcription repressor in *Arabidopsis thaliana* [21]. In the present experiment, we explored the underlying molecular mechanism of the CPN20 function, and showed that CPN20 antagonizes ABAR to relieve ABA-responsive WRKY40 transcription repressor of inhibition by ABAR in ABA signaling.

1 Materials and methods

1.1 Plant materials

Arabidopsis thaliana ecotype Col-0 was used as the wild-type control. The T-DNA insertion lines in the *CPN20* gene were all obtained from the Arabidopsis Biological Resource Center (ABRC). The mutant lines were genotyped by PCR and DNA gel-blot analysis as previously described [21]. The Col-0 plants were used to create *CPN20*-overexpressing transgenic lines as previously described [21]. The homozygous T3 seeds were used for further analysis. The *ABAR*-RNAi construct described previously [4] was used to transform the Col-0 plants to create *ABAR*-RNA lines as previously described [21]. The homologous T3 generation seeds or plants were used for analysis. The *cch cpn20-1* double mutants were generated by genetic crossing and identified by PCR genotyping. *Arabidopsis* seeds were disinfected and plated on MS medium (Sigma, St. Louis, USA) supplemented with 3% sucrose and 0.8% agar (pH 5.9), chilled for 3 d at 4°C and transferred to a growth chamber at ~80 μmol photons $m^{-2} s^{-1}$ or in compost soil at ~120 μmol photons $m^{-2} s^{-1}$ using cool white fluorescent lamps under a 16 h-light/8 h-dark photoperiod and 60% relative humidity.

1.2 Yeast two-hybrid assay

The Matchmaker Gal4 two-hybrid system (Clontech, Cambridge, USA) was used for yeast two-hybrid assays. The ORF of the middle fragment (encoding amino acid residues 348–1038) of *ABAR* was fused to GAL4 DNA binding domain in the plasmid pGBKT7. Yeast transformants were thoroughly selected on synthetic dropout medium (SD medium deficient in the nutrients Leu, Trp, His, and Ade) according to the manufacturer's instructions (Clontech, Cambridge, USA).

For analysis of protein interaction by two-hybrid assay, the full-length or partial sequences of *CPN20* were inserted into prey plasmid pGADT7 and the truncated *ABAR*s were cloned into bait plasmid pGBKT7. Primers used in the vector construction are presented in Table S1 in Supporting Information. Different combinations of plasmids were transformed into the yeast strain AH109. Transformants were plated on Leu-Trp-deficient and Leu-Trp-His-Ade-deficient medium separately and grew for 5–7 d at 30°C. The empty vectors pGBKT7 and pGADT7 were used as a negative control, while pGBKT-53 and pGADT7-T were used as a positive control. Expression of different fusion proteins was detected by immunoblot experiments. The ABARs-BD were analyzed using anti-Myc antibody and the CPN20s-AD were analyzed using anti-HA antibody.

1.3 β-galactosidase assay

The β-gal activity was quantitatively determined following the manufacturer's instructions (Clontech, Cambridge, USA). Cells were grown in liquid SD4- medium to an A_{600} of 0.5–0.8. Cells (1.5 mL) were pelleted, washed once in buffer Z (16.1 g L^{-1} $Na_2HPO_4 \cdot 7H_2O$, 5.5 g L^{-1} $NaH_2PO_4 \cdot H_2O$, 0.75 g L^{-1} KCl, 0.246 g L^{-1} $MgSO_4 \cdot 7 H_2O$, pH 7.0) and suspended in 300 μL of buffer Z. The cell suspension of 100 μL was lysed by three freeze/thaw cycles. Buffer Z (700 μL) containing 0.27% (v/v) 2-mercaptoeth- anol and 160 μL of 2-nitrophenyl-β-D-galactopyranoside (4 mg mL^{-1} in buffer Z) was added and incubated at 30°C. The sample was centrifuged after addition of 400 μL of 1 mol L^{-1} Na_2CO_3 and the A_{420} was measured. β-gal units were calculated as $1000 \times A_{420}/(A_{600} \times \text{min})$. Each value is the mean±SE of five independent biological determinations.

1.4 Production of anti-CPN20 serum

Production of the antibody against glutathione S-transferase (GST)-tagged CPN20 protein was described previously, and the affinity-purified anti-serum was evaluated by immunoblotting and shown to be highly specific to CPN20 [21].

1.5 Luciferase complementation imaging

Luciferase complementation imaging (LCI) assay was used to detect protein-protein interaction in *N. benthamiana* leaves according to previously described procedures [13,22]. The firefly luciferase (Luc) is divided into the N-terminal part (NLuc) and C-terminal part (CLuc). ABAR was fused with NLuc in pCAMBIA-NLuc vector, and CPN20, CPN20ΔNS or WRKY40 was fused with CLuc in pCAMBIA-CLuc vector respectively. Primers used for the vector construction are shown in Table S1 in Supporting Information. The constructs were mobilized into *A. tumefaciens* GV3101. Bacteria were suspended in infiltration buffer (0.2 mmol L^{-1} acetosyringone, 10 mmol L^{-1} $MgCl_2$, and 10 mmol L^{-1} MES) to identical concentrations (A_{600}=0.6). Equal concentrations and volumes of bacteria were mixed and co-infiltrated into the 7-week-old *N. benthamiana* leaves using needleless syringes. After infiltration, plants were placed with 16 h-light/8 h-dark for 48 h at 24°C. The

Luc activity was observed with a low-light cooled CCD imaging apparatus (Andor iXon, Belfast, UK). The mouse anti-full-length firefly Luc antibody (Santa Cruz Biotechnology, Texas, USA) was used to immunodetect Luc fusion protein in transgenic tissues. All experiments were repeated at least five independent biological replicates.

1.6 Three-hybrid assay and drop test of yeast growth

Yeast three-hybrid system (Clontech, Cambridge, USA) was applied to analyze the effect of CPN20 on the ABAR-WRKY40 interaction. The *WRKY40* cDNA was ligated into the prey plasmid pGADT7. The cDNA fragment encoding C-terminus (amino acid residues 692–1381) of ABAR was inserted into multiple cloning site I of the three-hybrid vector pBridge (Clontech, Cambridge, USA) downstream of the sequence of the GAL4 DNA binding domain. The full-length sequence or the truncated sequence with transit peptide and/or N-signature deletion of *CPN20* was inserted into multiple cloning site II under the control of a *MET25* promoter in the same pBridge vector. Primers used in this experiment are listed in Table S1 in Supporting Information. Activity of the *MET25* promoter can be inhibited in the presence of high concentrations of methionine, thus the expression levels of *CPN20* are able to be controlled by exogenous methionine. The construct pairs were co-transformed into yeast reporter strain AH109 according to the manufacturer's instructions (Clontech, Cambridge, USA). Transformants were plated on SD4- medium supplemented with or without 1 mmol L^{-1} methionine and incubated at 30°C for 5–7 d. Single colony of yeast cells was selected for the yeast growth assay.

In the drop test of yeast growth, yeast transformants grown on indicated SD4- medium were transferred into liquid SD4- with 1 mmol L^{-1} Met to A_{600}=0.2. *A* values were measured 4–5 h after incubation at 30°C. The cells were diluted in sterile water, and the diluted cells of 8 μL were spotted at the indicated concentrations (A_{600}=0.1, 0.01 and 0.001) on the SD4- with or without 1 mmol L^{-1} methionine. Images were taken 2 d after incubation at 30°C. *CPN20* was replaced by *GFP* in the pBridge vector as a control. Expression levels of the corresponding genes were analyzed by immunoblot assays. WRKY40 in the pGADT7 was detected by anti-HA serum, and ABAR and CPN20 in the pBridge were detected by anti-ABAR and anti-CPN20, respectively. The fluorescence of GFP protein was performed using fluorescence microscopy with the same settings (Olympus, BX51, Japan).

1.7 *In vitro* competitive pull-down assay

The full-length cDNA of *WRKY40* was ligated into the *Eco*R I and *Sal* I sites of pMAL-c2X vector. The *CPN20* cDNA was inserted into the *Eco*R I and *Sac* I sites of pET-48b vector. Primers used for these constructs are listed in Table S1 in Supporting Information. The WRKY40-MBP and CPN20-His fusion proteins were expressed in *Escherichia coli* BL21 (DE3) separately. Proteins were purified using amylose resin (for WRKY40-MBP) and NTA resin (for CPN20-His) as described in the manufacturer's system manual. The ABAR-His fusion protein was produced as previously described [12].

For competitive pull-down assays, ABAR-His (3 μg) with 1, 2 or 4 μg CPN20-His, or 4 μg BSA was incubated with 4 μg immobilized WRKY40-MBP at 4°C for 4 h. The amylose resin beads were washed with TBS buffer (50 mmol L^{-1} Tris-HCl, 150 mmol L^{-1} NaCl, 1% Triton X-100, pH 7.4) five times. The precipitated complexes were resolved and detected by immunoblotting with anti-ABAR antibody.

1.8 Real-time PCR analysis

Total RNA was isolated from 10-day-old seedlings using a Total RNA Rapid Extraction Kit (BioTeke), treated with RNase-free DNase I (TaKaRa, Japan) at 37°C for 30 min to degrade genomic DNA and purified by using an RNA Purification Kit (BioTeke, Beijing, China). A 2-μg aliquot of RNA was subjected to first-strand cDNA synthesis using M-MLV reverse transcriptase (Promega, Wisconsin, USA) and an oligo $d(T)_{18}$ primer. The primers used for real-time PCR are listed in Table S1 in Supporting Information. Analysis was performed using the BioRad Real-Time System CFX96TM C1000 Thermal Cycler (BioRad, California, USA). All experiments were repeated at least three times along with three independent repetitions of the biological experiments.

2 Results

2.1 ABA inhibits the CPN20-ABAR interaction

A previous study showed that CPN20 interacts with ABAR in ABA signaling [21]. In the present study, to investigate whether ABA affects the ABAR-CPN20 interaction, we used a fragment encoding the middle region of ABAR (amino acid residues (aa) 348–1038, abbreviated as $ABAR_{348–1038}$) as a bait to perform yeast two-hybrid assays as described previously [21]. Yeast drop test showed that the growth of yeast cells co-expressing CPN20 and $ABAR_{348–1038}$ was reduced on synthetic drop-out selection medium lacking Leu, Trp, His, and Ade (SD-Leu-Trp-His-Ade, SD4-) and supplemented with exogenous ABA (0.5 and 1 μmol L^{-1}, Figure 1A) in comparison with the transgenic yeast cells in the SD4- medium without ABA application (0 μmol L^{-1}, Figure 1A). This indicates that the ABA treatment decreases the ABAR-CPN20 interaction. Con-

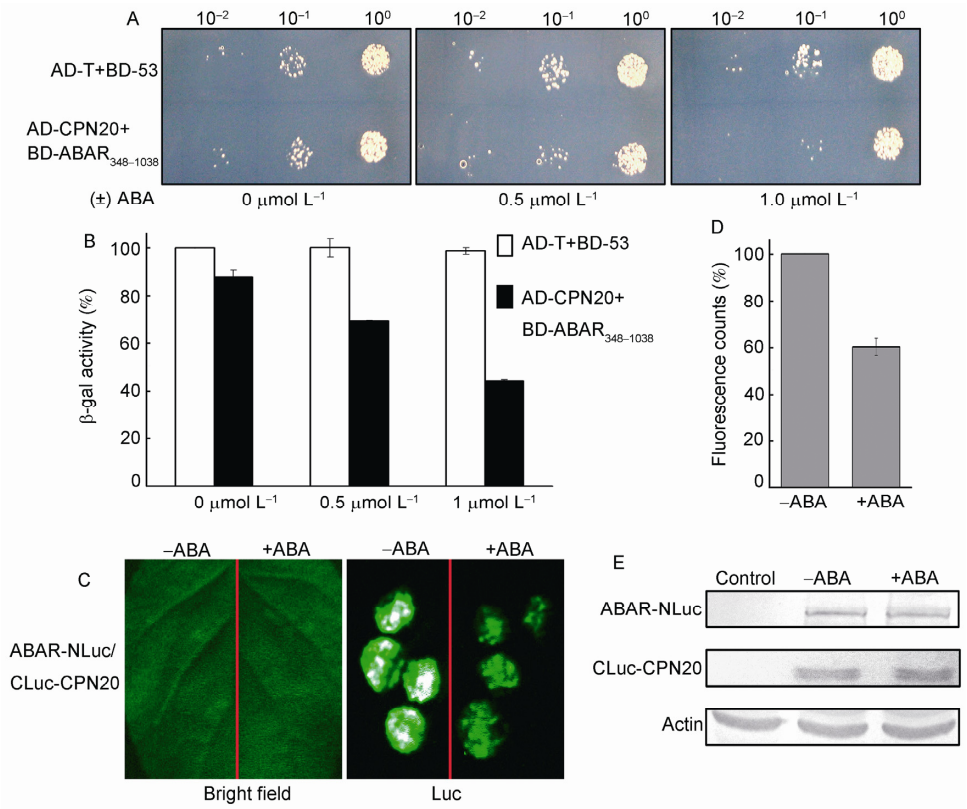

Figure 1 ABA inhibits the CPN20-ABAR interaction. A, Drop test assay in the yeast two-hybrid system: ABA treatment reduces the intensity of the interaction between ABAR and CPN20. The open reading frame (ORF) of the middle fragment (amino acid residues (aa) 348–1038) of *ABAR* was fused with the DNA binding domain in the bait vector pGBKT7 (BD-ABAR$_{348–1038}$), while the full-length sequence of *CPN20* was fused with activation domain in the prey vector pGADT7 (AD-CPN20). Yeast cells were cotransformed with the AD-CPN20/BD-ABAR$_{348–1038}$ construct pair, and were incubated in the SD medium lacking Leu, Trp, His, and Ade (SD4-) and containing 0, 0.5, or 1 μmol L^{-1} (±)ABA. Images were taken 2 d after the incubation. The yeast line harboring positive control vectors BD-53 plus AD-T was used as a control. B, Quantitative β-gal assay in the yeast two-hybrid system: ABA reduces the intensity of the interaction between ABAR and CPN20, which is indicated by decreased β-gal activity of the yeast lines harboring both ABAR and CPN20. The yeast line harboring vectors BD-53 plus AD-T was taken as a control. β-gal activity is presented as relative units (%), normalized relative to the activity of the yeast line harboring BD-53 and AD-T without ABA treatment (taken as 100%). Each value is the mean±SE of five independent biological determinations. C, Transient expression LCI assay in tobacco leaves: ABA treatment reduces the intensity of the ABAR-CPN20 interaction. Luminescence image is shown 48 h after co-infiltration with the construct pairs CLuc-CPN20/ABAR-NLuc with or without ABA treatment. "+ABA" indicates leaves infiltrated with 100 μmol L^{-1} (±)ABA for 4 h, while "–ABA" indicates leaves infiltrated with 0 μmol L^{-1} (±)ABA for 4 h. Left panel shows the bright-field image of the treated leaf. D, Quantitative analysis of the luminescence intensity in (C). The luminescence intensity without ABA treatment was taken as 100%. E, The protein amounts of CLuc-CPN20 and ABAR-NLuc in the tobacco leaves with or without ABA treatment described in (C), which were detected by immunoblotting using anti-CPN20 and anti-ABAR antiserum, respectively. The expression of *Actin* was used as an internal control. "Control" indicates leaves without transformation.

sistently, quantitative β-galactosidase activity assay confirmed that the intensity of the ABAR-CPN20 interaction was significantly reduced by different concentrations of exogenously applied ABA (Figure 1B). In the luciferase complementation imaging (LCI) assay, similar phenomenon was observed: ABA treatment obviously reduced the fluorescence intensity with the same expression levels of ABAR and CPN20 in the different treatments (Figure 1C–E), revealing that ABA represses the interaction between ABAR and CPN20 *in vivo*.

2.2 CPN20 inhibits ABAR-WRKY40 interaction by competitively binding to ABAR

Since both CPN20 and WRKY40 interact with ABAR and negatively regulate ABA signal transduction and CPN20 functions genetically upstream of WRKY40 and possibly at the same node with ABAR [13,21], we assumed that CPN20 functions in ABA signaling by modulating the ABAR-WRKY40 interaction. We used a combination of the pBridge yeast three-hybrid (Y3H) system, the LCI assay and competitive pull down assay to test this hypothesis.

To perform Y3H assays, we tested the domains of ABAR responsible for the CPN20-ABAR interaction to ensure that the domains used in the Y3H assays efficiently interact with both CPN20 and WRKY40. Previous studies showed that the C-terminal half of ABAR is essential for ABA signaling, which covers key functional domains to transmit ABA signal by interacting with a group of WRKY transcription factors [11,13]. Based on the hypothetical model of the

ABAR function, we divided ABAR into three fragments, $ABAR_{122–658}$ (aa 122–658), $ABAR_{631–999}$ (aa 631–999) and $ABAR_{941–1381}$ (aa 941–1381), to test which part of ABAR interacts with CPN20 by yeast two-hybrid assay. The results showed that the truncated form $ABAR_{631–999}$, instead of $ABAR_{122–658}$ or $ABAR_{941–1381}$, exhibits interaction with CPN20 in yeast (Figure S1 in Supporting Information). Interestingly, this region overlaps the "core of ABA-binding domain" in ABAR molecule [11].

Based on these above data, in the Y3H system, the truncated ABAR form $ABAR_{692–1381}$ was fused with the DNA binding domain, and CPN20 was fused with the MET25 promoter that could be conditionally regulated by different concentrations of methionine (Met) in the pBridge vector (pBridge-$ABAR_{692–1381}$-CPN20). WRKY40 was fused with the DNA activating domain in the pGADT7 vector (AD-WRKY40). The ABAR-WRKY40 interaction was measured by yeast drop tests and β-galactosidase activity assays in the AH109 yeast cells co-transformed with pBridge-$ABAR_{692–1381}$-CPN20 and AD-WRKY40. We observed that the growth of yeast cells harboring pBridge-$ABAR_{692–1381}$-CPN20 and AD-WRKY40 was significantly reduced when the yeast cells were plated in SD4- without exogenous Met (allowing high expression of *CPN20*), in comparison with the growth of yeast cells plated in SD4- supplemented with 1 mmol L^{-1} Met (repressing expression of *CPN20*) (Figure 2A–C). The expression levels of $ABAR_{692–1381}$ and WRKY were not significantly changed in the yeast cells (Figure 2C), showing that the altered intensity of the ABAR-WRKY40 interaction was not caused by possible changes in the amounts of the proteins. Additionally, no significant difference in the yeast growth was detected when *CPN20* was replaced by *GFP* in the pBridge vector (a negative control, Figure 2A, B and D), and the results of β-galactosidase activity analysis were consistent with those of the growth of yeast cells (Figure 2A and B). In the LCI assay, the fluorescence signal was significantly reduced when CPN20 was co-expressed with ABAR-NLuc and CLuc-WRKY40, whereas the fluorescence intensity was not altered when GFP was co-expressed with ABAR-NLuc and CLuc-WRKY40 in the leaves of tobacco (Figure 2E and F). The expression levels of ABAR and WRKY40 were not significantly changed in the tobacco cells (Figure 2G), showing that the altered intensity of the ABAR-WRKY40 interaction was not caused by possible changes in the amounts of the proteins. Furthermore, we confirmed the antagonistic effect of CPN20 on the ABAR-WRKY40 interaction in the competitive pull down assay: CPN20 reduced the amounts of WRKY40-pulled-down ABAR protein in a dose-dependent manner (Figure 2H). All these findings reveal that CPN20 inhibits the interaction between ABAR and WRKY40 by competitively binding to ABAR.

2.3 CPN20 interacts with ABAR via its N-signature domain

CPN20 consists of two CPN10-like domains, which share 46% amino acid identity to each other. Both units contain a highly conserved signature sequence (the PLXDRVL amino acid residues) and a mobile loop region [23]. To investigate which domain is responsible for the interaction with ABAR, we divided CPN20 into nine corresponding fragments named CPN20C1, CPN20C2, CPN20C3, CPN20C4, CPN20N1, CPN20N2, CPN20N3, CPN20N4 and CPN20N5 (Figure 3A), to test which domain is responsible for the interaction with $ABAR_{631–999}$ in yeast cells. The result showed that the CPN20N5 (aa 1–91) containing N-signature sequence and N-mobile loop region, CPN20N4 (aa 1–74) and CPN20N3 (aa 1–70) both containing N-signature sequence only, interact with $ABAR_{631–999}$ (Figure 3A and B). However, neither CPN20C3 (aa 75–253) composed of two mobile loop regions and the C-signature sequence, nor CPN20C2 (aa 150–253) composed of C-mobile loop region and C-signature sequence, exhibit interaction with $ABAR_{631–999}$ (Figure 3A and B). These data suggest that the highly conserved N-signature domain in the N-terminus of CPN20 is one of the essential domains responsible for the interaction of CPN20 with ABAR protein.

2.4 Deletion of N-signature of CPN20 abolishes its ability to inhibit ABAR-WRKY40 interaction

We further tested whether disruption of the interaction between ABAR and CPN20 affects the ABAR-WRKY40 interaction. As described earlier, deletion of the N-signature from the CPN20 disrupts the CPN20-ABAR interaction (Figure 3). We showed that, in contrast to the full-length CPN20, the truncated CPN20 with deletion of its N-signature (CPN20C3, Figure 4A) lost the capacity to inhibit the interaction between ABAR and WRKY40 in the yeast three-hybrid system (Figure 4B). This observation was confirmed in the tobacco LCI system (Figure 4C–E). The N-signature was deleted from, but the chloroplast transit peptide was linked to, the CPN20 molecule, forming a truncated CPN20 (CPN20ΔNS). The CPN20ΔNS showed no ability to reduce the ABAR-WRKY40 interaction (Figure 4C and D). The expression levels of ABAR, CPN20 (including full-length CPN20 and CPN20ΔNS) and WRKY were not significantly changed in the tobacco leaves (Figure 4E), showing that the altered intensity of the ABAR-WRKY40 interaction was not caused by possible changes in the amounts of the proteins. These findings provide further evidence for the above-described observation that CPN20 inhibits the interaction between ABAR and WRKY40.

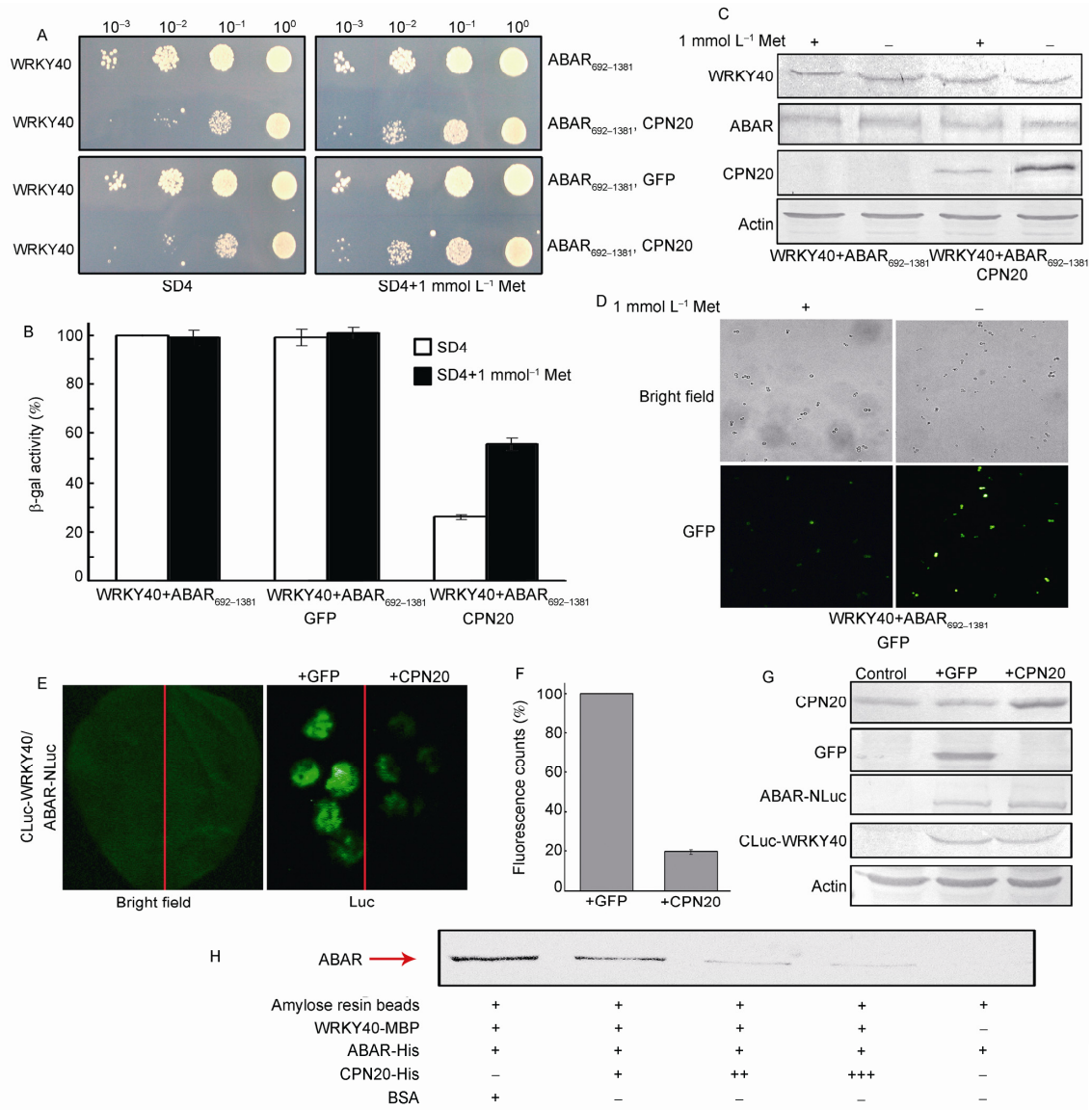

Figure 2 CPN20 antagonizes the interaction between ABAR and WRKY40. A, CPN20 antagonizes the interaction between ABAR and WRKY40 *in vitro*: drop test assay of the yeast three-hybrid system. The cDNA fragment encoding the C-terminus (amino acid residues 692–1381) of ABAR was inserted into multiple cloning site I of the three-hybrid vector pBridge downstream of the sequence of the GAL4 DNA binding domain, and the full-length sequence of *CPN20* was inserted into multiple cloning site II under the control of a *MET25* promoter in the same pBridge vector, which was indicated by "$ABAR_{692-1381}$, CPN20". WRKY40 was fused with activation domain in the vector pGADT7, which was indicated by "WRKY40". CPN20 was replaced by GFP in the pBridge-$ABAR_{692-1381}$-CPN20 vector, which was indicated by "$ABAR_{692-1381}$, GFP". Yeast cells co-transformed with the different combinations of construct pairs were incubated in the SD medium lacking Leu, Trp, His and Ade (SD4-) appending 0 (–) or 1 (+) mmol L^{-1} methionine (Met). Images were taken 2 d after the incubation. The yeast lines harboring vectors pBridge-$ABAR_{692-1381}$ plus AD-WRKY40 and vectors pBridge-$ABAR_{692-1381}$-GFP plus AD-WRKY40 were used as controls. B, The β-gal assays used to quantify the intensity of the interactions described in (A). β-gal activity is presented as relative units (%), normalized relative to the activity of the yeast line harboring pBridge-$ABAR_{692-1381}$ and AD-WRKY40 in the SD medium lacking Leu, Trp, His and Ade appending 0 mmol L^{-1} Met (SD4) (taken as 100%). Each value is the mean±SE of five independent biological determinations. C, Immunoblot analysis of WRKY40, $ABAR_{692-1381}$ and CPN20 proteins expressed in the yeast strains described in (A). Total proteins were extracted from the yeast strains and analyzed by immunoblotting using anti-HA , anti-ABAR and anti-CPN20, respectively. D, Test of the expression of GFP in the yeast strains described in (A) by fluorescence microscopy. Top panels, the bright-field images of the yeast strains incubated in the SD medium lacking Leu, Trp, His and Ade and appending 0 (–) or 1 (+) mmol L^{-1} Met. Bottom panels, the fluorescence of GFP corresponding to the top panel. E, CPN20 antagonizes the interaction between ABAR and WRKY40 *in vivo*. The tobacco leaf was co-transformed with ABAR-NLuc/CLuc-WRKY40 appending CPN20 (+CPN20) or GFP (+GFP) (right panel). The left panel shows the bright field of the treated leaf. F, Quantitative analysis of luminescence intensity in (E). The luminescence intensity obtained from ABAR-NLuc/CLuc-WRKY40 appending GFP was taken as 100%. All the assays were repeated five times with similar results. Error bars represent SE. G, The protein amounts of CPN20, GFP, CLuc-WRKY40 and ABAR-NLuc in the tobacco leaves detected by immunoblotting using anti-CPN20, anti-GFP, anti-CLuc and anti-ABAR serums, respectively. "Control" indicates leaves without transformation. The expression of *Actin* was used as an internal control. H, Pull down assay: interaction between ABAR-His and WRKY40-MBP is antagonized by CPN20-His. ABAR-His and BSA or different amounts of CPN20-His were incubated with immobilized WRKY40-MBP. The ABAR-His protein was detected by anti-ABAR antibody. "–" indicates no addition; "+" indicates addition; "++" indicates addition with doubled amounts.

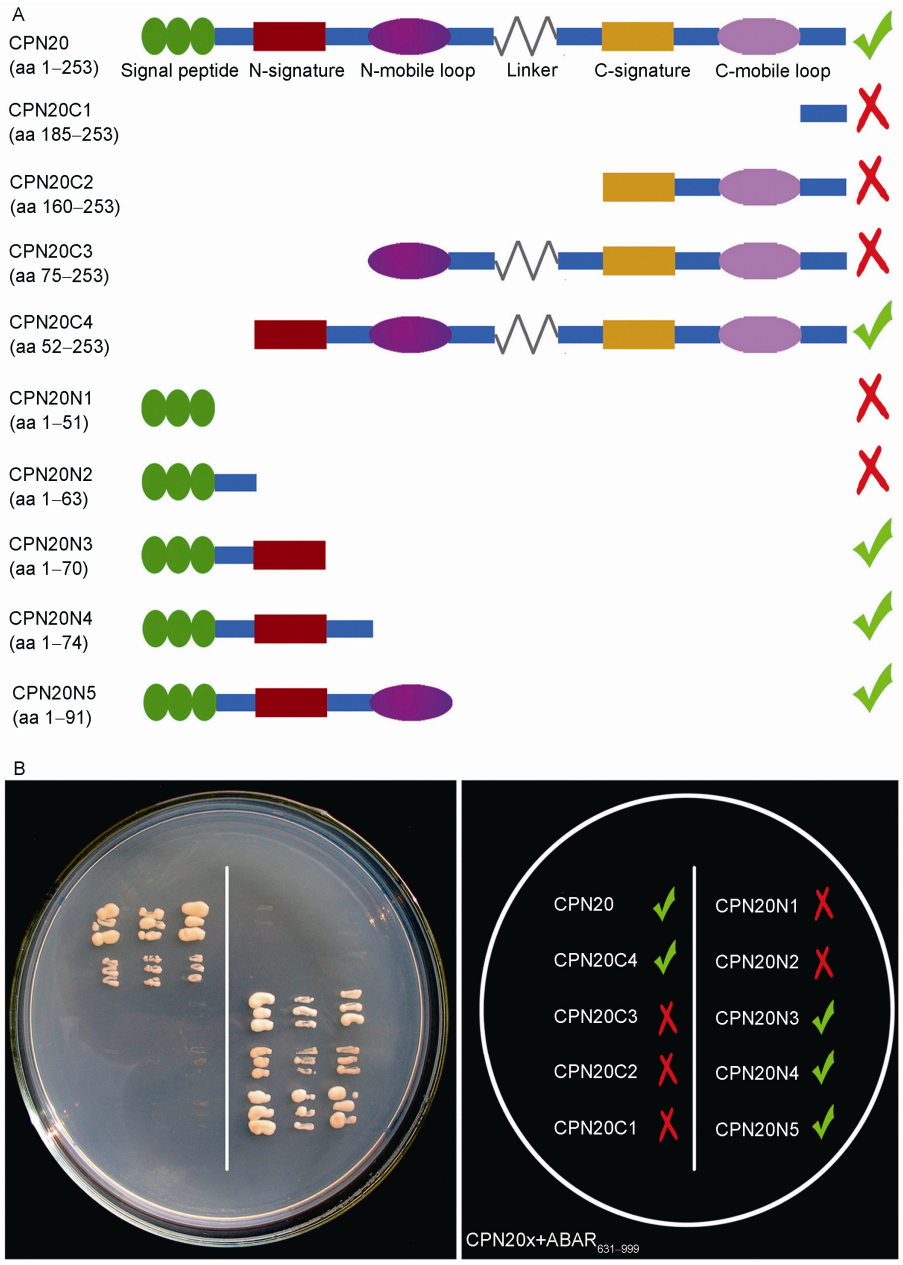

Figure 3 The N-signature of CPN20 is responsible for the CPN20-ABAR interaction. A and B, The assays in yeast two-hybrid assays using $ABAR_{631–999}$ as a bait. CPN20 was divided into nine different fragments, which are indicated in (A). These fragments fused with DNA activating domain were individually co-transformed with BD-$ABAR_{631–999}$ into yeast cells, and specific interactions were observed with the following AD-constructs: CPN20C4, CPN20N3, CPN20N4, CPN20N5 (B). The green symbol "right (√)" indicates occurrence of interaction and the red symbol "wrong (×)" indicates no interaction. The experiments were repeated three times with the same results.

2.5 Genetic evidence that CPN20 antagonizes ABAR to positively regulate *WRKY40* expression

Previous reports showed that ABAR antagonizes the WRKY40 transcription factor by repressing *WRKY40* expression in response to ABA [13], and the above experiments support that CPN20 may function in ABA signaling by inhibiting the ABAR-WRKY40 interaction (Figures 2–4). To further support this idea with genetic data, we tested whether expression of the *WRKY40* gene was altered when the expression levels of the *CPN20* gene were changed. We observed that *WRKY40* was significantly downregulated in *cpn20-1* and *cpn20-2* mutants, but upregulated in the *CPN20*-overexpression line (Figure 5A and B). Whereas *WRKY40* was significantly upregulated in *cch* mutant, introduction of *cpn20* mutation into *cch* mutant suppressed the *WRKY40*-upregulation in the *cch* mutant: *cpn20 cch* double mutant showed reduced *WRKY40* level like *cpn20-1* or *cpn20-2* (Figure 5B). These data show that the homeostasis of the *WRKY40* expression requires both

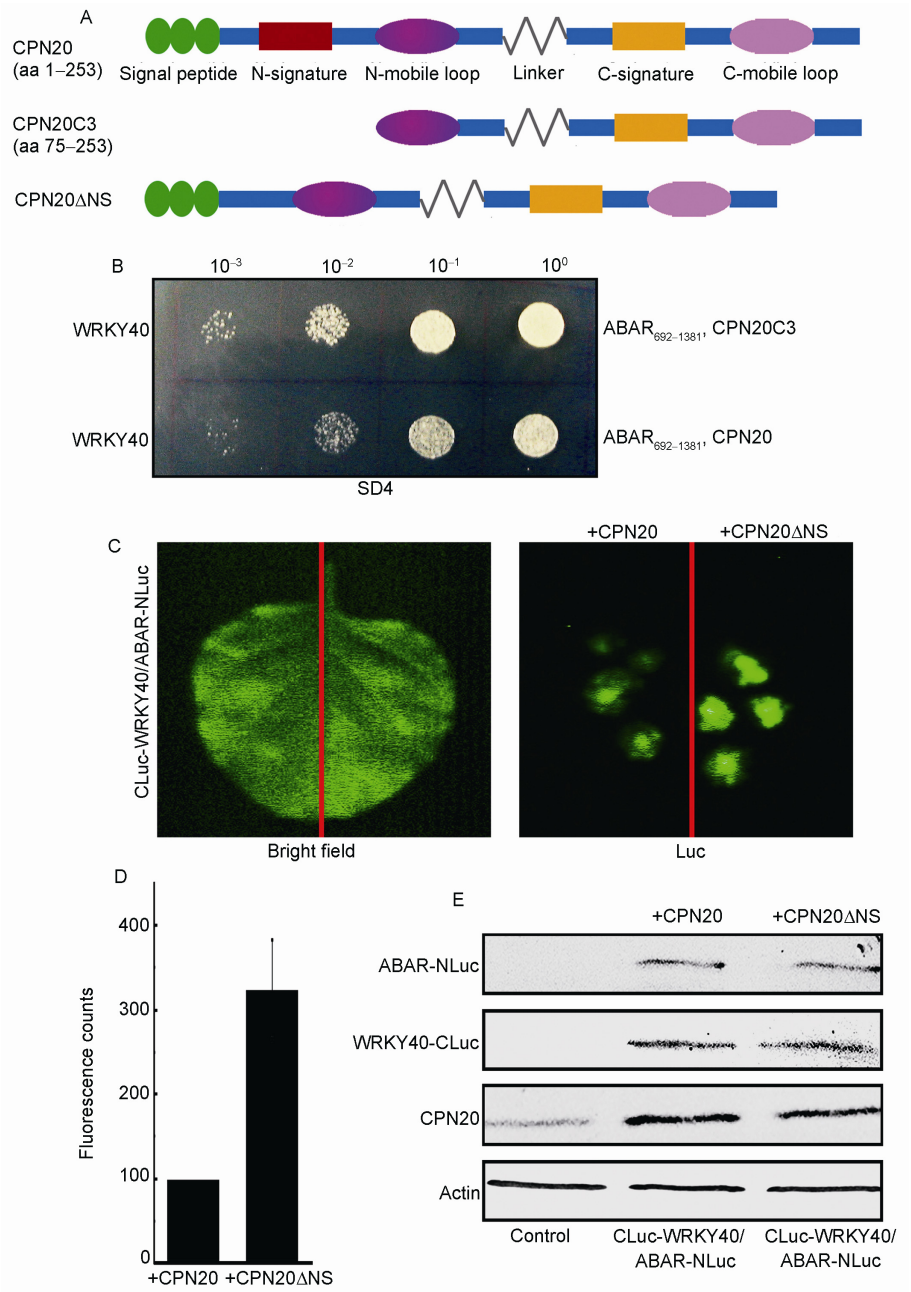

Figure 4 Deletion of the CPN20-N-signature suppresses the repressive effect of CPN20 on ABAR-WRKY40 interaction. A, Truncated CPN20 used in the bimolecular interactions. CPN20C3, truncated CPN20 with signal peptide and N-signature deletion; CPN20ΔNS, truncated CPN20 only with N-signature deletion. B, Drop test assay in the yeast three-hybrid system: CPN20, but not CPN20C3, reduces the intensity of the interaction between ABAR and WRKY40. Yeast cells were cotransformed with the AD-WRKY40 and pBridge-ABAR-CPN20/CPN20C3 construct pair, and were incubated in the SD medium lacking Leu, Trp, His, and Ade (SD4). Images were taken 2 d after the incubation. The assays were repeated five times with similar results. C, Transient expression LCI assay in tobacco leaves: CPN20, but not CPN20ΔNS, reduces the intensity of the interaction between ABAR and WRKY40. Luminescence image (right panel) is shown 48 h after co-infiltration with the construct pairs CLuc-WRKY40/ABAR-NLuc and together with CPN20 or CPNB20ΔNS. Left panel shows the bright-field image of the treated leaf. D, Fluorescence counts of the tobacco leaves described in (C). The value from the "+CPN20" was taken as 100%, and that from the "+CPN20ΔNS" was normalized relative to this value. The assays were repeated five times with similar results. Error bars represent SE. E, The immunoblotting-detected protein amounts of CLuc-WRKY40, ABAR-NLuc and CPN20 in the tobacco leaves described in (C). The expression of *Actin* was used as an internal control. "Control" indicates leaves without transformation.

ABAR and CPN20, and support the notion that CPN20, like ABAR, functions upstream of WRKY40 [13,21].

Next, we tested whether the ABA responsiveness of the *WRKY40* expression was altered in the *cpn20* mutant. As previously described [13,15], ABA treatment reduces the *WRKY40* expression level, and this repressive effect depends at least partly on ABAR, given that the *WRKY40* level was enhanced but the repressive effect of ABA on

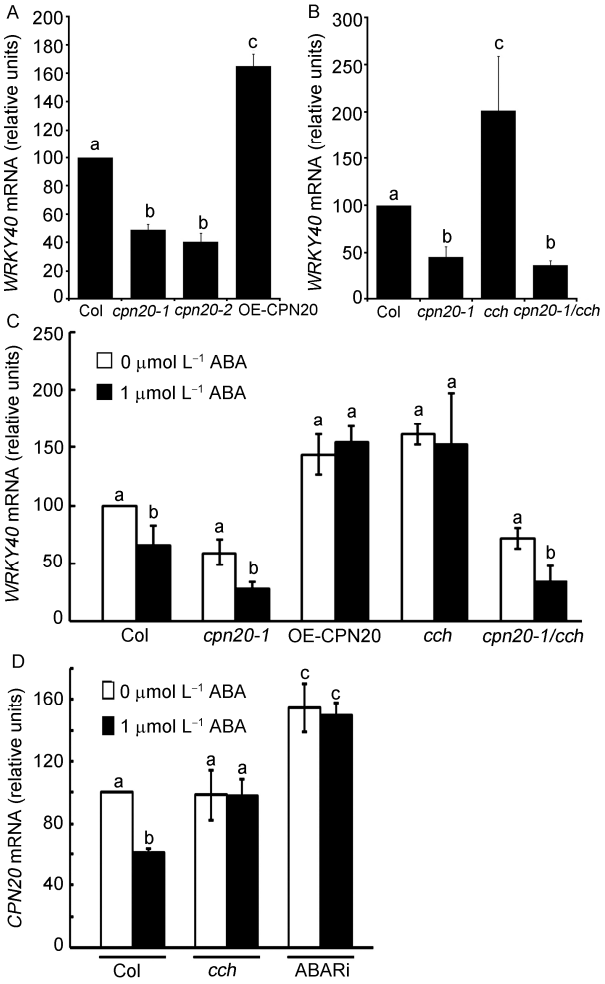

Figure 5 Expression of *WRKY40* gene is altered in *cpn20*, *CPN20*-overexpression and *cpn20 cch* mutants. The real-time PCR analysis was performed with two-week-old seedling. A, Expression of *WRKY40* in the wild-type Col, *cpn20* mutants and a *CPN20*-overexpression line (OE-CPN20). Each value is the mean±SE of three biological determinations, and different letters indicate significant differences at $P<0.05$ (Duncan's multiple-range test) when the WRKY40 expression levels are compared among different genotypes. B, Expression of *WRKY40* in the wild-type Col, *cpn20-1*, *cch* single mutants and *cpn20-1 cch* double mutant. Each value is the mean±SE of three biological determinations, and different letters indicate significant differences at $P<0.05$ (Duncan's multiple-range test) when the WRKY40 expression levels are compared among different genotypes. C, Expression of *WRKY40* in the wild-type Col, *cpn20-1*, *cch* single mutants, *cpn20 cch* double mutant and a *CPN20*-overexpression line (OE-CPN20). For 1 μmol L^{-1} ABA treatment, seeds were directly planted in the ABA-containing medium and seedlings were sampled two weeks after stratification. Each value is the mean±SE of three biological determinations, and different letters indicate significant differences at $P<0.05$ (Student's *t*-test) when the *WRKY40* expression levels are compared between 0 and 1 μmol L^{-1} ABA treatments within the same genotype. D, Expression of *CPN20* in the wild-type Col, *cch* mutant and an *ABAR*-RNAi line (ABARi). The ABA treatment was done as described above in (C). Each value is the mean±SE of three biological determinations, and different letters indicate significant differences at $P<0.05$ (Duncan's multiple-range test) when the *CPN20* expression levels are compared between 0 and 1 μmol L^{-1} ABA treatments and among different genotypes.

WRKY40 gene was reduced in the *cch* mutant (Figure 5C). Interestingly, we observed that the repressive effect of ABA on *WRKY40* expression was enhanced in *cpn20* mutant, which contrasts with the observation in *cch* mutant (Figure 5C), while the *cpn20-1 cch* double mutant showed the *cpn20* mutant phenotype (Figure 5C). We further found that the *CPN20* expression was inhibited by ABA treatment, but this inhibitory effect of ABA on *CPN20* was lost in the *cch* mutant (Figure 5D). The *CPN20* expression was enhanced in an *ABAR*-RNAi line downregulating the *ABAR* gene expression (Figure 5D). Taken together, these data suggest that CPN20 antagonizes ABAR to positively regulate *WRKY40* expression, and in turn, the *CPN20* expression is negatively regulated by ABAR likely by a complicated feed-back effect in response to ABA.

3 Discussion

Previous studies showed that ABAR directly interacts and antagonizes the WRKY40 transcription repressor, a negative ABA signaling regulator, which inhibits a set of ABA-responsive genes involved in ABA-induced physiological responses [13–15]. Most recently, we identified CPN20 as another interaction partner of ABAR, which is, like WRKY40, negatively involved in ABA signaling [21]. Together with the previously reported genetic data [21], we provided compelling evidence that CPN20 antagonizes ABAR to derepress the WRKY40 transcription repressor. First, ABA directly inhibits the ABAR-CPN20 interaction (Figure 1), and also represses expression of *CPN20*, which depends on ABAR (Figure 5), revealing that ABA may inhibit the ABAR-CPN20 interaction by reducing the CPN20 number via ABAR and directly acting on the ABAR-CPN20 bimolecular interaction. Second, CPN20 inhibits ABAR-WRKY40 interaction by competitively binding to ABAR (Figures 2–4). These data provide biochemical evidence that CPN20 functions through antagonizing the ABAR-WRKY40 coupled pathway, and ABA relieves this pathway of repression by inhibiting the ABAR-CPN20 interaction to activate ABAR-WRKY40 interaction. Third, previously reported genetic evidence clearly demonstrates that CPN20 functions at the same node with ABAR but upstream of WRKY40 transcription repressor in ABA signaling pathway [21]. Last, gene expression analysis reveals that ABAR downregulates, but CPN20 upregulates, WRKY40 expression, and the *cpn20-1* mutation induces downregulation of *WRKY40*, which suppresses the upregulated level of *WRKY40* due to the *cch* mutation (Figure 5), supporting the notion that CPN20 functions at the same node with ABAR but upstream of WRKY40 transcription repressor. Additionally and importantly, we previously showed that ABA inhibits *WRKY40* expression in wild-type plants [13,15], and we found in the present study that this inhibitory effect of ABA is strengthened by downregulation of *CPN20* but reduced by upregulation of *CPN20* (Figure 5). These data reveal that CPN20 activates *WRKY40*

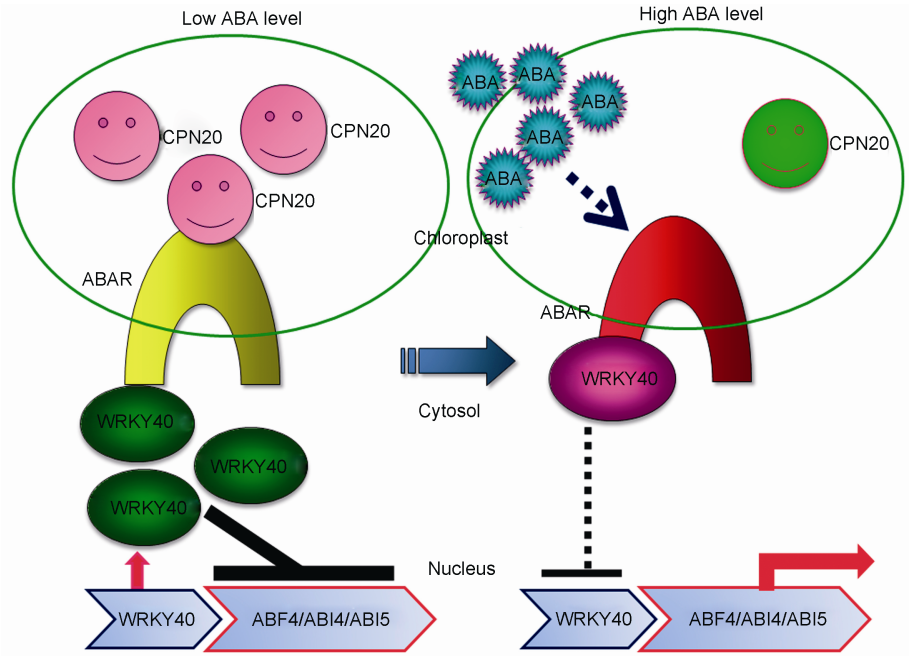

Figure 6 A working model of CPN20 in ABA signaling pathway. CPN20 interacts with ABAR tightly at low ABA level. The interaction of CPN20 with ABAR at low ABA level attenuates the interaction between ABAR and WRKY40, which aids to maintain a suitable level of WRKY40 that represses ABA-responsive genes; high level of ABA inhibits the ABAR-CPN20 interaction, which in turn promotes the ABAR-WRKY40 interaction that triggers downstream signaling to repress *WRKY40* expression, resulting in de-repressing the ABA-responsive genes. See detailed explanation in the text. Arrows denote positive regulation or activation, and bars negative regulation or repression. The solid lines indicate direct effect and dotted lines indirect effect.

expression antagonistically to ABAR. All the data are consistent with the idea that ABA signal, through interacting with ABAR, antagonizes CPN20 to repress its negative function in ABA signaling.

A working model of the CPN20-ABAR-WRKY40 signaling cascades is proposed based on these data (Figure 6). In this model, CPN20 interacts with ABAR tightly at low ABA level, which attenuates the interaction between ABAR and WRKY40. A previous report showed that the ABA-activated ABAR-WRKY40 interaction triggers a yet unknown downstream signaling component/cascade to repress *WRKY40* expression [13]. Thus, the inhibition of the ABAR-WRKY40 interaction is favourable to keeping a high level of WRKY40 to repress ABA-responsive genes. High level of ABA inhibits the ABAR-CPN20 interaction, which in turn promotes the ABAR-WRKY40 interaction to trigger the downstream signaling to repress WRKY40 expression. The decrease in amounts of WRKY40 in nucleus relieves ABA-responsive genes of inhibition, which finally induces ABA-related physiological responses. Further studies will be needed to explore the novel players to elucidate the unknown signaling nodes in this ABA signaling pathway.

Accession numbers

Sequence data from this article can be found in the Arabidopsis Genome Initiative Database under the following accession numbers: *CPN20* (AT5G20720), *ABAR/CHLH* (At5g13630), *WRKY40* (At1g80840). Germplasm identification numbers for mutant lines are as follows: *cpn20*-1 (SAIL_888_A09), *cpn20*-2 (SALK_083054C), *wrky40*-1 (stock number: ET5883, Cold Spring Harbor Laboratory gene and enhancer trap lines).

The cpn20 mutant seeds were provided by the ABRC. We thank Dr. Liu Dong (Tsinghua University, Beijing, China) for help on materials. This work was supported by the National Key Basic Research Program of China (2012CB114302), National Natural Science Foundation of China (90817104 and 31170268), and Ministry of Agriculture of China (2013ZX08009-003).

1 Finkelstein RR, Gampala S, Rock C. Abscisic acid signaling in seeds and seedlings. Plant Cell, 2002, 14: S15–45
2 Adie BAT, Perez-Perez J, Perez-perez MM, Godoy M, Sanchez-Serrano JJ, Schmelz EA, Solanoa R. ABA is an essential signal for plant resistance to pathogens affecting JA biosynthesis and the activation of defenses in *Arabidopsis*. Plant Cell, 2007, 19: 1665–1681
3 Cutler SR, Rodriguez PL, Finkelstein RR, Abrams SR. Abscisic acid: emergence of a core signaling network. Annu Rev Plant Bio, 2010, 61: 651–679
4 Shen YY, Wang XF, Wu FQ, Du SY, Cao Z, Shang Y, Wang XL, Peng CC, Yu XC, Zhu SY, Fan RC, Xu YH, Zhang DP. The Mg-chelatase H subunit is an abscisic acid receptor. Nature, 2006, 443: 823–826
5 Liu XG, Yue YL, Li W, Ma LG. Response to comment on a G protein coupled receptor is a plasma membrane receptor for the plant hormone abscisic acid. Science, 2007a, 318: 914
6 Liu XG, Yue YL, Li B, Nie YL, Li W, Wu WH, Ma LG. A G protein-coupled receptor is a plasma membrane receptor for the plant hormone abscisic acid. Science, 2007b, 315: 1712–1716
7 Ma Y, Szostikiewicz I, Korte A, Moes D, Yang Y, Christman A,

Grill E. Regulators of PP2C phosphatase activity function as abscisic acid sensors. Science, 2009, 324: 1064–1068
8 Pandey S, Nelson DC, Assmann SM. Two novel GPCR-type G proteins are abscisic acid receptors in *Arabidopsis*. Cell, 2009, 136: 136–148
9 Park SY, Fung P, Nishimura N, Jensen DR, Fujii H, Zhao Y, Lumba S, Santiago J, Rodrigues A, Chow TF, Alfred SE, Bonetta D, Finkelstein R, Provart NJ, Desveaux D, Rodriguez PL, McCourt P, Zhu JK, Schroeder JI, Volkman BF, Cutler SR. Abscisic acid inhibits type 2C protein phosphatases via the PYP/PYL family of START proteins. Science, 2009, 324: 1068–1071
10 Santiago J, Rodrigues A, Saez A, Rubio S, Antoni R, Dupeux F, Park SY, Marquez JA, Culter SR, Rodriguez PL. Modulation of drought resistance by the abscisic acid receptor PYL5 through inhibition of clade A PP2Cs. Plant J, 2009, 60: 575–588
11 Wu FQ, Xin Q, Cao Z, Liu ZQ, Du SY, Mei C, Zhao CX, Wang XF, Shang Y, Jiang T, Zhang XF, Yan L, Zhao R, Cui ZN, Liu R, Sun HL, Yang XL, Su Z, Zhang DP. The Mg-chelatase H subunit binds abscisic acid and functions in abscisic acid signaling: new evidence in *Arabidopsis*. Plant Physiol, 2009, 150: 1940–1954
12 Du SY, Zhang XF, Lu Z, Xin Q, Wu Z, Jiang T, Lu Y, Wang XF, Zhang DP. Roles of the different components of magnesium chelatase in abscisic acid signal transduction. Plant Mol Bio, 2012, 80: 519–537
13 Shang Y, Yan L, Liu ZQ, Cao Z, Mei C, Xin Q, Wu FQ, Wang XF, Du SY, Jiang T, Zhang XF, Zhao R, Sun HL, Liu R, Yu YT, Zhang DP. The Mg-chelatase H subunit antagonizes a group of WRKY transcription repressors to relieve ABA-responsive genes of inhibition. Plant Cell, 2010, 22: 1909–1935
14 Liu ZQ, Yan L, Wu Z, Mei C, Wang XF, Zhang DP. Cooperation of three WRKY-domain transcription factors WRKY18, WRKY40 and WRKY60 in repressing two ABA-responsive genes *ABI4* and *ABI5* in *Arabidopsis*. J Exp Bot, 2012, 63: 6371–6392
15 Yan L, Liu ZQ, Xu YH, Lu K, Wang XF, Zhang DP. Auto- and cross-repression of three *Arabidopsis* WRKY transcription factors WRKY18, WRKY40 and WRKY60 negatively involved in ABA signaling. J Plant Growth Regul, 2013, 32: 399–416
16 Tsuzuki T, Takahashi K, Inoue SI, Okigaki Y, Tomiyama M, Hossain MA, Shimazaki KI, Murata Y, Kinoshita T. Mg-chelatase H subunit affects ABA signaling in stomatal guard cells, but is not an ABA receptor in *Arabidopsis thaliana*. J Plant Res, 2011, 124: 527–538
17 Wang XF, Xin Q, Shen YY, Zhang DP. Approaches to the identification of ABAR as an abscisic acid receptor. In: Kermode AR, ed. Seed Dormancy: Methods in Molecular Biology. New York: Springer Science+Business Media, LLC, 2011. 83–97
18 Legnaioli T, Cuevas J, Mas P. TOC1 functions as a molecular switch connecting the circadian clock with plant responses to drought. EMBO J, 2009, 28: 3745–3757
19 Jia HF, Chai YM, Li CL, Qin L, Shen YY. Cloning and characterization of the H subunit of a magnesium chelatase gene (*PpCHLH*) in peach. J Plant Growth Regul, 2011a, 30: 445–455
20 Jia HF, Chai YM, Li CL, Lu D, Luo JJ, Qin L, Shen YY. Abscisic acid plays an important role in the regulation of strawberry fruit ripening. Plant Physiol, 2011b, 157: 188–199
21 Zhang XF, Jiang T, Wu Z, Du SY, Yu YT, Jiang SC, Lu K, Feng XJ, Wang XF, Zhang DP. Cochaperonin CPN20 negatively regulates abscisic acid signaling in *Arabidopsis*. Plant Mol Biol, 2013, 83: 205–218
22 Chen H, Zou Y, Shang Y, Lin H, Wang Y, Cai R, Tang X, Zhou JM. Firefly luciferase complementation imaging assay for protein-protein interactions in plants. Plant Physiol, 2008, 146: 368–376
23 Weiss C, Bonshtien A, Farchi-Pisanty O, Vitlin A. Cpn20: Siamese twins of the chaperonin world. Plant Mol Biol, 2009, 69: 227–238

Supporting Information

Figure S1 Test of interaction of truncated ABARs with CPN20 in yeast two-hybrid system.

Table S1 Primers used in this study

The supporting information is available online at life.scichina.com and link.springer.com. The supporting materials are published as submitted, without typesetting or editing. The responsibility for scientific accuracy and content remains entirely with the authors.